Publishing House
AKAPIT

COMPUTER METHODS IN MATERIALS SCIENCE
Informatyka w Technologii Materiałów

Vol. 17, 2017, No. 2

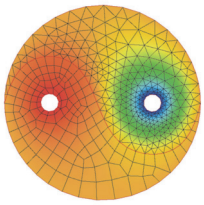

STRUCTURE-PRESERVING NUMERICAL SCHEME FOR A GENERALIZED AREA-PRESERVING CRYSTALLINE CURVATURE FLOW

Tetsuya Ishiwata[1], **Shigetoshi Yazaki**[2,*]

[1] *College of Systems Engineering and Science, Shibaura Institute of Technology, 307 Fukasaku, Minuma-ku, Saitama 337-8570, Japan*
[2] *School of Science and Technology, Meiji University, 1-1-1 Higashi-Mita, Tama-ku, Kanagawa 214-8571, Japan*
[*] *Corresponding author: syazaki@meiji.ac.jp*

Abstract

The presented numerical scheme preserves variational structure of a generalized area-preserving crystalline curvature flow. The scheme is based on an iteration and a projection method. Several numerical examples will verify that the enclosed area is preserved in numerical computation with high accuracy in the sense of double precision. Numerical computations realize theoretical convexification results starting from almost convex polygon, and are extended to a general setting starting from nonconvex polygon.

Key words: structure-preserving, area-preserving crystalline curvature flow, iteration, convexification, negative crystal, accurate numerical computation

1. INTRODUCTION

Crystalline curvature flows have been extensively studied from the mathematical as well as from the numerical point of view. They are strong singular anisotropic curvature flows, so that moving curves are restricted as in an admissible class associated with the Wulff shape. This strategy of restriction was founded by Angenent and Gurtin (1989) and Taylor (1991). Besides such restrictions, several constrained curvature driven flows have been also interested, which include area-preserving curvature flows, Hele-Shaw flows, surface diffusion flows, etc. Area-preserving crystalline curvature flows are regarded as crystalline curvature flows under keeping the enclosed area surrounded by closed curves in the plane. These flows come from not only mathematical interests, but also from modeling of motion of vapor figures or negative crystals (Ishiwata & Yazaki, 2007, 2008, 2017). From the modeling view point, one of the purpose of this paper is to give mathematical justification of Nakaya's observation for the evolution process of vapor figures in the ice block (Nakaya, 1956), and realize the Nakaya's experimental observation numerically for the ice block in the heat gradient field (Nakaya, 1956). Practically, we construct an accurate numerical scheme for area-preserving crystalline curvature flows, which is an extended scheme by Ushijima and Yazaki (2004) and Beneš et al. (2009).

Let Γ be the polygonal Jordan curve in the plane with N-vertices labeled $\boldsymbol{x}_1, \boldsymbol{x}_2, \cdots, \boldsymbol{x}_N$ ($\boldsymbol{x}_0 = \boldsymbol{x}_N, \boldsymbol{x}_{N+1} = \boldsymbol{x}_1$) in the anti-clockwise order, and let Γ_i be the i-the edge $\Gamma_i = [\boldsymbol{x}_{i-1}, \boldsymbol{x}_i]$ ($i = 1, 2, \cdots, N$). The following two constructions are basic of crystalline setting.

ISSN 1641-8581

Construction 1 ($\boldsymbol{x} \Rightarrow r, \boldsymbol{t}, \boldsymbol{n}, h, \nu$)**.** Several quantities on Γ_i are defined and derived from $\{\boldsymbol{x}_i\}_{i=0}^{N+1}$ as follows ($i = 1, 2, \cdots, N$):

- $r_i = |\boldsymbol{x}_i - \boldsymbol{x}_{i-1}|$: the length of Γ_i;
- $\boldsymbol{t}_i = \dfrac{\boldsymbol{x}_i - \boldsymbol{x}_{i-1}}{r_i}$: the tangent vector on Γ_i;
- $\boldsymbol{n}_i = -\boldsymbol{t}_i^{\perp}$ the outward normal vector on Γ_i, where $\begin{pmatrix} a \\ b \end{pmatrix}^{\perp} = \begin{pmatrix} -b \\ a \end{pmatrix}$;
- $h_i = \boldsymbol{x}_i \cdot \boldsymbol{n}_i = \boldsymbol{x}_{i-1} \cdot \boldsymbol{n}_i$: the hight function for Γ_i;
- ν_i: the tangent angle satisfying $\boldsymbol{t}_i = (\cos\nu_i, \sin\nu_i)^{\mathrm{T}}$, where $(a, b)^{\mathrm{T}} = \begin{pmatrix} a \\ b \end{pmatrix}$. All tangent angles $\{\nu_i\}_{i=0}^{N+1}$ can be derived as in the following procedure: Firstly, from $\boldsymbol{t}_1 = (t_{11}, t_{12})^{\mathrm{T}}$, we have $\nu_1 = -\arccos(t_{11})$ if $t_{12} < 0$; $\nu_1 = \arccos(t_{11})$ if $t_{12} \geq 0$. Secondly, for $i = 1, 2, \cdots, N$, we successively compute ν_{i+1} from ν_i as $\nu_{i+1} = \nu_i + (\operatorname{sgn} D) \arccos I$, where $D = \det(\boldsymbol{t}_i, \boldsymbol{t}_{i+1})$ and $I = \boldsymbol{t}_i \cdot \boldsymbol{t}_{i+1}$. Finally, we obtain $\nu_0 = \nu_1 - (\nu_{N+1} - \nu_N)$, since $\nu_N = \nu_0 + 2\pi$ and $\nu_{N+1} = \nu_1 + 2\pi$ hold;
- $\phi_i = \nu_{i+1} - \nu_i$: the i-th external angle between Γ_i and Γ_{i+1}.

Note that all the quantities except $\{\nu_i\}_{i=0}^{N+1}$ satisfy the periodic boundary conditions: $\mathsf{F}_0 = \mathsf{F}_N, \mathsf{F}_{N+1} = \mathsf{F}_1$.

Construction 2 ($h, \nu \Rightarrow \boldsymbol{x}, \boldsymbol{t}, \boldsymbol{n}, r$)**.** Conversely, the set of vertices $\{\boldsymbol{x}_i\}_{i=1}^{N}$ can be constructed from the sets $\{h_i\}_{i=1}^{N+1}$ ($h_{N+1} = h_1$) and $\{\nu_i\}_{i=1}^{N+1}$ ($\nu_{N+1} = \nu_1 + 2\pi$) as follows. Let $\boldsymbol{t}(\nu) = (\cos\nu, \sin\nu)^{\mathrm{T}}$ and $\boldsymbol{n}(\nu) = (\sin\nu, -\cos\nu)^{\mathrm{T}}$, and then we have $\boldsymbol{t}_i = \boldsymbol{t}(\nu_i)$ and $\boldsymbol{n}_i = \boldsymbol{n}(\nu_i)$. Since $h_i = \boldsymbol{x}_i \cdot \boldsymbol{n}(\nu_i)$ and $h_{i+1} = \boldsymbol{x}_i \cdot \boldsymbol{n}(\nu_{i+1})$, from the sets $\{h_i\}_{i=1}^{N+1}$ and $\{\nu_i\}_{i=1}^{N+1}$ we obtain

$$\begin{pmatrix} \boldsymbol{n}(\nu_i)^{\mathrm{T}} \\ \boldsymbol{n}(\nu_{i+1})^{\mathrm{T}} \end{pmatrix} \boldsymbol{x}_i = \begin{pmatrix} h_i \\ h_{i+1} \end{pmatrix}, \quad \text{where } \begin{pmatrix} a \\ b \end{pmatrix}^{\mathrm{T}} = (a, b).$$

Therefore

$$\boldsymbol{x}_i = \frac{h_{i+1}\boldsymbol{t}_i - h_i\boldsymbol{t}_{i+1}}{\sin\phi_i}, \quad \phi_i = \nu_{i+1} - \nu_i \qquad (1)$$

hold for $i = 1, 2, \cdots, N$. From this the length of the i-th edge can be described as

$$r_i = \frac{h_{i+1}}{\sin\phi_i} - h_i(\cot\phi_i + \cot\phi_{i-1}) + \frac{h_{i-1}}{\sin\phi_{i-1}}.$$

For N-tuples $\boldsymbol{h} = (h_1, h_2, \cdots, h_N)$ and $\boldsymbol{\phi} = (\phi_1, \phi_2, \cdots, \phi_N)$ with the periodic boundary conditions $\mathsf{F}_0 = \mathsf{F}_N, \mathsf{F}_{N+1} = \mathsf{F}_1$, we denote the right hand side of r_i as $D_i(\boldsymbol{h}, \boldsymbol{\phi})$, i.e.,

$$r_i = D_i(\boldsymbol{h}, \boldsymbol{\phi}) \qquad (2)$$

holds for $i = 1, 2, \cdots, N$.

The Wulff polygon and admissibility. Now let us restrict the polygonal curve Γ in an admissible class associated with the N_σ-sided convex polygon, say the Wulff polygon W_σ for an appropriate positive function σ:

$$W_\sigma = \bigcap_{i=1}^{N_\sigma} \{\boldsymbol{x} \in \mathbb{R}^2 ; \boldsymbol{x} \cdot \boldsymbol{n}(\eta_i) \leq \sigma(\eta_i)\},$$

where η_i is the tangent angle of the i-th edge of W_σ ($i = 1, 2, \cdots, N_\sigma$). Such σ is called crystalline interfacial energy density. The length of the i-th edge is described as

$$l_\sigma(\eta_i) = D_i(\boldsymbol{\sigma}(\eta), \boldsymbol{\psi}),$$

where

$$\boldsymbol{\sigma}(\eta) = (\sigma(\eta_1), \sigma(\eta_2), \cdots, \sigma(\eta_{N_\sigma})),$$
$$\boldsymbol{\psi} = (\psi_1, \psi_2, \cdots, \psi_{N_\sigma}),$$

and $\psi_i = \eta_{i+1} - \eta_i \in (0, \pi)$ for $i = 1, 2, \cdots, N_\sigma$ ($\psi_0 = \psi_{N_\sigma}$, $\psi_{N_\sigma+1} = \psi_1$). Note that $\sigma > 0$ should be satisfied $l_\sigma(\eta_i) > 0$ for $i = 1, 2, \cdots, N_\sigma$. Let $\mathcal{N} = \{\boldsymbol{n}_i\}_{i=1}^{N}$ and $\mathcal{N}_\sigma = \{\boldsymbol{n}(\eta_j)\}_{j=1}^{N_\sigma}$ be the set of normal vectors on Γ and ∂W_σ, respectively. The polygonal curve Γ is called W_σ-admissible if the following two conditions are satisfied.

1. $\mathcal{N} \subset \mathcal{N}_\sigma$;
2. $\dfrac{(1-\lambda)\boldsymbol{n}_i + \lambda\boldsymbol{n}_{i+1}}{|(1-\lambda)\boldsymbol{n}_i + \lambda\boldsymbol{n}_{i+1}|} \notin \mathcal{N}_\sigma$ for $i = 1, 2, \cdots, N$ ($\boldsymbol{n}_{N+1} = \boldsymbol{n}_1$) and $\lambda \in (0, 1)$.

Let $\Gamma(t)$ be the W_σ-admissible, N-sided and time t-dependent polygonal curve. The curve $\Gamma(t) = \bigcup_{i=1}^{N} \Gamma_i(t)$, $\Gamma_i(t) = [\boldsymbol{x}_{i-1}(t), \boldsymbol{x}_i(t)]$ evolves by prescribed normal velocities:

$$v_i = \dot{\boldsymbol{x}}_i \cdot \boldsymbol{n}(\nu_i) = \dot{h}_i \quad (i = 1, 2, \cdots, N),$$

which will be defined later. Here and hereafter, $\dot{\mathsf{F}} = d\mathsf{F}/dt$ means the derivative w.r.t. time. Note that for any ϕ_i there is a $j \in \{1, 2, \cdots, N_\sigma\}$ such that $|\phi_i| = \psi_j$ holds.

The energy and the crystalline curvature. The total length and the total interfacial energy are defined as

$$L = \sum_{i=1}^{N} r_i, \quad L_\sigma = \sum_{i=1}^{N} \sigma(\nu_i) r_i.$$

Since the time differential of $r_i = D_i(\boldsymbol{h}, \phi)$ is

$$\dot{r}_i = D_i(\dot{\boldsymbol{h}}, \phi) = D_i(\boldsymbol{v}, \phi), \quad \boldsymbol{v} = (v_1, \cdots, v_N),$$

the time differential of L and L_σ are

$$\dot{L} = \sum_{i=1}^{N} \dot{r}_i = \sum_{i=1}^{N} D_i(\boldsymbol{v}, \phi) = \sum_{i=1}^{N} v_i D_i(\mathbf{1}, \phi) = \\ = \sum_{i=1}^{N} k_i v_i r_i,$$

$$\dot{L}_\sigma = \sum_{i=1}^{N} \sigma(\nu_i) D_i(\boldsymbol{v}, \phi) = \sum_{i=1}^{N} v_i D_i(\boldsymbol{\sigma}(\nu), \phi) = \\ = \sum_{i=1}^{N} k_{\sigma i} v_i r_i,$$

respectively, where

$$k_i = \frac{D_i(\mathbf{1}, \phi)}{r_i}, \quad D_i(\mathbf{1}, \phi) = \tan\frac{\phi_i}{2} + \tan\frac{\phi_{i-1}}{2}, \\ \mathbf{1} = (1, \cdots, 1),$$

$$k_{\sigma i} = \frac{D_i(\boldsymbol{\sigma}(\nu), \phi)}{r_i}, \quad D_i(\boldsymbol{\sigma}(\nu), \phi) = \chi_i l_\sigma(\nu_i), \\ \chi_i = \frac{1}{2}(\mathrm{sgn}(\phi_{i-1}) + \mathrm{sgn}(\phi_i)), \\ \boldsymbol{\sigma}(\nu) = (\sigma(\nu_1), \sigma(\nu_2), \cdots, \sigma(\nu_N)).$$

The k_i and the $k_{\sigma i}$ are called the i-th polygonal curvature and the i-th crystalline curvature, respectively, and the χ_i is called the i-th transition number.

The area and the gradient flow. The time differential of enclosed area $A = \frac{1}{2}\sum_{i=1}^{N} h_i r_i$ is

$$\dot{A} = \frac{1}{2}\sum_{i=1}^{N}\left(\dot{h}_i r_i + h_i \dot{r}_i\right) = \frac{1}{2}\sum_{i=1}^{N}\left(v_i r_i + h_i D_i(\boldsymbol{v}, \phi)\right) \\ = \frac{1}{2}\sum_{i=1}^{N}\left(v_i r_i + v_i D_i(\boldsymbol{h}, \phi)\right) = \sum_{i=1}^{N} v_i r_i.$$

Hence the area-preserving gradient flow of L_σ can be calculated from

$$\dot{L}_\sigma + \lambda \dot{A} = \sum_{i=1}^{N} (k_{\sigma i} + \lambda) v_i r_i,$$

and we have $v_i = -k_{\sigma i} - \lambda$. The Lagrange multiplier λ is determined as $\lambda = -\frac{L_\sigma}{L}$ from $\dot{A} = 0$. Consequently, we obtain the area-preserving crystalline curvature flow equations

$$v_i = \frac{L_\sigma}{L} - k_{\sigma i} \quad (i = 1, 2, \cdots, N). \tag{3}$$

Now we are ready to set up the problem. Let P_σ^N be a set of all W_σ-admissible, N-sided polygonal Jordan curve in the plane.

Problem. For a given $\Gamma_0 \in P_\sigma^N$ find a family of curves $\{\Gamma(t) \in P_\sigma^N\}_{0 \le t < T}$ satisfying

$$\begin{cases} \dot{h}(t) = v_i(t) \quad (i = 1, 2, \cdots, N), \\ \Gamma(0) = \Gamma_0. \end{cases}$$

When the normal velocities $\{v_i\}_{i=1}^N$ are given by (3), the problem is a system of ODEs, and its can be solved locally in time, i.e., as long as $r_i > 0$ holds for all i. Moreover under the following three assumptions, edge-disappearing phenomena occurs in the sense of the following result.

(A0) W_σ is an N_σ-sided symmetric polygon with respect to the origin.

(A1) $\Gamma_0 \in P_\sigma^N$ holds with $N > N_\sigma$.

(A2) Transition numbers of Γ_0 are all nonnegative: $\chi_i \ge 0$ $(i = 1, 2, \cdots, N)$.

Theorem A (Ishiwata & Yazaki (2017)) *Assume that the assumptions* (A0), (A1) *and* (A2). *Then there exists $T_1 > 0$ such that the solution polygon $\Gamma(t) \in P_\sigma^N$ holds for $0 \le t < T_1$ and there exists at least one edge with zero transition number whose length tends to zero as $t \to T_1$. Moreover, $\Gamma(t)$ converges to $\Gamma' \in P_\sigma^{N'}$ $(N_\sigma \le N' < N)$ in the Hausdorff metric as $t \to T_1$ and enclosed area of Γ' is equal to enclosed area of Γ_0.*

In the case where $N' > N_\sigma$ holds, the result of Theorem A will be repeated, that is, there exists $T_2 > T_1$ such that a solution polygon $\Gamma(t)$ starting with the initial polygon Γ' evolves until time T_2 and the same phenomena as in Theorem A occur as t tends to T_2. After the time T_2, since number of edges is finite, edge-disappearing occurs at most finitely many instants

$$0 < T_1 < T_2 < \cdots < T_m,$$

and eventually the solution polygon becomes an convex polygon belonging to $P_\sigma^{N_\sigma}$ at the final time $t = T_m$. In the case $N' = N_\sigma$, the final time T_m is T_1 and the polygon Γ' belongs to $P_\sigma^{N_\sigma}$ and is convex. In

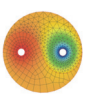

any cases, after the above "convexity phenomena" occurred, the solution polygon converges the boundary of a Wulff shape which is homothetically the same shape of W_σ as time tends to infinity (Yazaki, 2008) by using the anisoperimetric inequality or Brünn and Minkowski's inequality and the theory of dynamical systems which is the similar technique as in the paper of isotropic version (Yazaki 2002). The results were extended when Γ_0 was essentially admissible polygon (Yazaki, 2007).

Generalization. We generalize the area-preserving crystalline curvature flow in an inhomogeneous weighted field such as

$$v_i = \langle\varepsilon\rangle_i \left(\frac{\sum_{j=1}^N \langle\varepsilon\rangle_j k_{\sigma j} r_j}{\sum_{j=1}^N \langle\varepsilon\rangle_j r_j} - k_{\sigma i} \right) \quad (i = 1, 2, \cdots, N), \tag{4}$$

where $\varepsilon(\boldsymbol{x})$ is a positive function for $\boldsymbol{x} \in \mathbb{R}^2$ and

$$\langle\varepsilon\rangle_i = \frac{1}{r_i} \int_{\Gamma_i} \varepsilon(\boldsymbol{x})\, ds$$

is the average of $\varepsilon(\boldsymbol{x})$ on Γ_i. In the present paper, we use practically $\varepsilon(\bar{\boldsymbol{x}}_i)$ instead of $\langle\varepsilon\rangle_i$, where

$$\bar{\boldsymbol{x}}_i = \frac{\boldsymbol{x}_i + \boldsymbol{x}_{i-1}}{2}$$

is the mid-point of Γ_i. It is easy to check that the area-preserving property

$$\dot{A} = 0$$

holds and the energy-decreasing property

$$\dot{L}_\sigma \le 0$$

holds by using the CBS inequality. The equality holds if and only if $k_{\sigma i} = const.$ holds for all i. By the closedness of Γ and anti-clockwise labeling of $\{\boldsymbol{x}_i\}_{i=1}^N$, the $const.$ should be positive, so that $\chi_i = 1$ and $\dfrac{l_\sigma(\nu_i)}{r_i} = const. > 0$ hold for all i, which means that $N = N_\sigma$ and Γ is homothetically the same as the boundary of the Wulff shape W_σ.

In what follows, we present the numerical test of Theorem A and solve the general problem numerically when the normal velocities $\{v_i\}_{i=1}^N$ are given by (4).

2. NUMERICAL SCHEME

When the normal velocities $\{v_i\}_{i=1}^N$ are given by (4), according to Ushijima and Yazaki (2004) and Beneš et al. (2009), the evolution equations $\dot{h}_i = v_i$ $(i = 1, 2, \cdots, N)$ can be discretized such as

$$\frac{h_i^{m+1} - h_i^m}{\tau_m} = \varepsilon_i^m \left(\frac{\sum_{j=1}^N \varepsilon_j^m k_{\sigma j}^{m+1/2} r_j^{m+1/2}}{\sum_{j=1}^N \varepsilon_j^m r_j^{m+1/2}} - k_{\sigma i}^{m+1/2} \right) \quad (i = 1, 2, \cdots, N), \tag{5}$$

where h_i^m is an approximation of $h_i(t_m)$ at the m-th time $t_m = \sum_{i=0}^{m-1} \tau_i$ $(m = 1, 2, \cdots;\ t_0 = 0)$, and $\varepsilon_i^m = \varepsilon(\bar{\boldsymbol{x}}_i^m)$, $\bar{\boldsymbol{x}}_i^m = \dfrac{\boldsymbol{x}_i^m + \boldsymbol{x}_{i-1}^m}{2}$, where $\boldsymbol{x}_i^m$ is an approximation of $\boldsymbol{x}_i(t_m)$. The quantities at the $(m+1/2)$-th time step in (5) are approximations evaluated at the time $t_{m+1/2} = t_m + \dfrac{\tau_m}{2}$. The m-th time increment $\tau_m > 0$ will be determined later.

Scheme. Let $\Gamma^0 = \bigcup_{i=1}^N [\boldsymbol{x}_{i-1}^0, \boldsymbol{x}_i^0] \in P_\sigma^N$ be a given initial polygonal Jordan curve $(\boldsymbol{x}_0^0 = \boldsymbol{x}_N^0, \boldsymbol{x}_{N+1}^0 = \boldsymbol{x}_1^0)$. For the time step $m = 0, 1, 2, \cdots$ the $(m+1)$-th polygonal Jordan curve $\Gamma^{m+1} = \bigcup_{i=1}^N [\boldsymbol{x}_{i-1}^{m+1}, \boldsymbol{x}_i^{m+1}] \in P_\sigma^N$ $(\boldsymbol{x}_0^{m+1} = \boldsymbol{x}_N^{m+1}, \boldsymbol{x}_{N+1}^{m+1} = \boldsymbol{x}_1^{m+1})$ is computed successively as long as $\min\limits_{1 \le i \le N} r_i^m > 0$ holds as follows:

1. Compute $r_i^m, \boldsymbol{t}_i^m, \boldsymbol{n}_i^m, h_i^m, \nu_i^m, \varepsilon_i^m$ from $\{\boldsymbol{x}_j^m\}_{j=1}^N$ by Construction 1 $(i = 1, 2, \cdots, N)$;
2. Solve (5), and obtain $\{h_i^{m+1}\}_{i=1}^N$;
3. Compute $\boldsymbol{x}_i^{m+1}, \boldsymbol{t}_i^{m+1}, \boldsymbol{n}_i^{m+1}, r_i^{m+1}$ from $\{h_j^{m+1}\}_{j=1}^N$ and $\{\nu_j^{m+1}\}_{j=1}^N$ by Construction 2 $(i = 1, 2, \cdots, N)$;
4. Put $m := m + 1$ and GOTO (1);

Note that $\nu_i^{m+1} = \nu_i^m$ holds for $i = 1, 2, \cdots, N$ as long as $\Gamma^m \in P_\sigma^N$ holds $(m = 0, 1, 2, \cdots)$.

How to solve (5). Since $\nu_i^{m+1} = \nu_i^m$ holds for $i = 1, 2, \cdots, N$, we have $\chi_i^{m+1} = \chi_i^m$ and $\phi_i^{m+1} = \phi_i^m$ for all i. Therefore, the tangential angle at the $(m + 1/2)$-th time step is $\nu_i^{m+1/2} = \dfrac{\nu_i^{m+1} + \nu_i^m}{2} = \nu_i^m$, and then

$$\begin{aligned} k_{\sigma i}^{m+1/2} r_i^{m+1/2} &= D_i(\boldsymbol{\sigma}(\nu^{m+1/2}), \boldsymbol{\phi}^{m+1/2}) \\ &= D_i(\boldsymbol{\sigma}(\nu^m), \boldsymbol{\phi}^m) = \chi_i^m l_\sigma(\nu_i^m), \\ \chi_i^m &= \frac{\mathrm{sgn}(\phi_{i-1}^m) + \mathrm{sgn}(\phi_i^m)}{2} \end{aligned}$$

hold for $i = 1, 2, \cdots, N$, where $\boldsymbol{\sigma}(\nu^j) = (\sigma(\nu_1^j), \cdots, \sigma(\nu_N^j))$ and $\boldsymbol{\phi}^j = (\phi_1^j, \cdots, \phi_N^j)$.

We define the i-th hight function and the length of edge at the $(m+1/2)$-th time step by

$$h_i^{m+1/2} = \frac{h_i^{m+1} + h_i^m}{2}$$

and

$$r_i^{m+1/2} = D_i(\boldsymbol{h}^{m+1/2}, \boldsymbol{\phi}^{m+1/2}),$$

respectively, for $i = 1, 2, \cdots, N$, where $\boldsymbol{h}^j = (h_1^j, \cdots, h_N^j)$. Then we have

$$\begin{aligned} r_i^{m+1/2} &= D_i(\boldsymbol{h}^{m+1/2}, \boldsymbol{\phi}^{m+1/2}) = D_i(\boldsymbol{h}^{m+1/2}, \boldsymbol{\phi}^m) \\ &= \frac{D_i(\boldsymbol{h}^{m+1}, \boldsymbol{\phi}^m) + D_i(\boldsymbol{h}^m, \boldsymbol{\phi}^m)}{2} \\ &= \frac{r_i^{m+1} + r_i^m}{2} \end{aligned}$$

for $i = 1, 2, \cdots, N$.

Let the right-hand-side of (5) be

$$\begin{aligned} F_i(\boldsymbol{h}^{m+1/2}) &:= F_i(\boldsymbol{h}^{m+1/2}; \boldsymbol{h}^m, \boldsymbol{\sigma}(\nu^m), \boldsymbol{\phi}^m, \boldsymbol{\varepsilon}^m) \\ &= \varepsilon_i^m \left(\frac{\sum_{j=1}^N \varepsilon_j^m k_{\sigma j}^{m+1/2} r_j^{m+1/2}}{\sum_{j=1}^N \varepsilon_j^m r_j^{m+1/2}} - k_{\sigma i}^{m+1/2} \right), \\ k_{\sigma i}^{m+1/2} &= \frac{D_i(\boldsymbol{\sigma}(\nu^m), \boldsymbol{\phi}^m)}{r_i^{m+1/2}}, \\ r_i^{m+1/2} &= D_i(\boldsymbol{h}^{m+1/2}, \boldsymbol{\phi}^m), \end{aligned}$$

for $i = 1, 2, \cdots, N$, where $\boldsymbol{\varepsilon}^m = (\varepsilon_1^m, \varepsilon_2^m, \cdots, \varepsilon_N^m)$. We solve

$$h_i^{m+1/2} = h_i^m + F_i(\boldsymbol{h}^{m+1/2}) \frac{\tau_m}{2} \quad (i = 1, 2, \cdots, N)$$

by the iteration as the following steps.

1. $l = 0$; $\boldsymbol{y}^{(l)} = \boldsymbol{h}^m$;
2. $\boldsymbol{y}^{(l+1)} = \boldsymbol{h}^m + \boldsymbol{F}(\boldsymbol{y}^{(l)})\tau_m/2$;
3. If $||\boldsymbol{y}^{(l+1)} - \boldsymbol{y}^{(l)}||/r_{\max}^m \le \delta_{\rm tol}$, then GOTO (5);
4. $l := l + 1$; GOTO (2);
5. $\boldsymbol{h}^{m+1} = R^{(l+1)}\widetilde{\boldsymbol{y}}^{(l+1)}$, $\widetilde{\boldsymbol{y}}^{(l+1)} = 2\boldsymbol{y}^{(l+1)} - \boldsymbol{h}^m$.

Here $\delta_{\rm tol} > 0$ is a tolerance, $R^{(j)}$ is a rescaling sequence which will be defined later (10),

$$\boldsymbol{y}^{(j)} = (y_1^{(j)}, \cdots, y_N^{(j)}), \ \boldsymbol{F}(\boldsymbol{y}^{(j)}) = (F_1(\boldsymbol{y}^{(j)}), \cdots, F_N(\boldsymbol{y}^{(j)})), \ \widetilde{\boldsymbol{y}}^{(j)} = (\widetilde{y}_1^{(j)}, \cdots, \widetilde{y}_N^{(j)}),$$

$||\boldsymbol{y}^{(l+1)} - \boldsymbol{y}^{(l)}|| = \max_{1 \le i \le N} |y_i^{(l+1)} - y_i^{(l)}|$ and hereafter we denote $\mathsf{F}_{\max} = \max_{1 \le i \le N} \mathsf{F}_i$.

How to determine τ_m. Let $z_i^{(l)} = D_i(\boldsymbol{y}^{(l)}, \boldsymbol{\phi}^m)$ for $i = 1, 2, \cdots, N$ and $l = 0, 1, 2, \cdots$. Then we have

$$z_i^{(0)} = D_i(\boldsymbol{y}^{(0)}, \boldsymbol{\phi}^m) = D_i(\boldsymbol{h}^m, \boldsymbol{\phi}^m) = r_i^m \quad (i = 1, 2, \cdots, N),$$

and obviously

$$\begin{aligned} &z_i^{(0)} \le z_{\max}^{(0)} = r_{\max}^m < (1+c) r_{\max}^m \\ \text{and} \quad &z_i^{(0)} \ge z_{\min}^{(0)} = r_{\min}^m > (1-c) r_{\min}^m \end{aligned} \tag{6}$$

hold for $c \in (0, 1)$ and $i = 1, 2, \cdots, N$. Here and hereafter we denote $\mathsf{F}_{\min} = \min_{1 \le i \le N} \mathsf{F}_i$.

We determine the m-th time increment τ_m such as

$$\tau_m = \lambda_m \frac{c(1-c)^2 (r_{\min}^m)^2}{c_\sigma^m} \tag{7}$$

for $c \in (0, 1)$ and $m = 0, 1, 2, \cdots$, where

$$a_\sigma = \min_{1 \le i \le N_\sigma} \sin \psi_i,$$

$$b_\sigma = \max_{1 \le i \le N_\sigma} l_\sigma(\eta_i),$$

$$c_\sigma^m = \frac{4 b_\sigma \varepsilon_{\max}^m}{a_\sigma}$$

are positive constants determined by the Wulff shape W_σ, and

$$\lambda_m = \min \left\{ \frac{1}{2}, \ \frac{2\varepsilon_{\max}^m A^m}{a_\sigma (1-c^2) r_{\min}^m r_{\max}^m S_\varepsilon^m} \right\} \in (0, 1),$$

Here $S_\varepsilon^m = \sum_{j=1}^N \varepsilon_j^m$ and

$$A^m = \frac{1}{2} \sum_{i=1}^N h_i^m r_i^m$$

is the enclosed area of Γ^m.

Under the time increment (7), the following proposition holds.

Proposition 2.1 *Let $\boldsymbol{z}^{(l)} = (z_1^{(l)}, z_2^{(l)}, \cdots, z_N^{(l)})$ for $l = 0, 1, 2, \cdots$. For $m = 0, 1, 2, \cdots$ and $c \in (0, 1)$ we have the followings.*

$$(1)\ (1-c) r_{\min}^m \le z_i^{(l)} \le (1+c) r_{\max}^m \quad (i = 1, 2, \cdots, N;\ l = 0, 1, 2, \cdots).$$

$$(2)\ ||\boldsymbol{z}^{(l+1)} - \boldsymbol{z}^{(l)}|| \le c ||\boldsymbol{z}^{(l)} - \boldsymbol{z}^{(l-1)}|| \quad (l = 1, 2, \cdots).$$

$$(3)\ \lim_{l \to \infty} y_i^{(l)} = h_i^{m+1/2} \quad \textit{and} \quad \lim_{l \to \infty} z_i^{(l)} = r_i^{m+1/2} \quad (i = 1, 2, \cdots, N).$$

Here $||\boldsymbol{z}^{(j)} - \boldsymbol{z}^{(j-1)}|| = \max_{1 \le i \le N} |z_i^{(j)} - z_i^{(j-1)}|$ for $j = 1, 2, \cdots$.

Proof. In this proof, we use the estimate $\lambda_m \le 1$ in (7).

(1) The inequalities are proved by mathematical induction on l. For $l = 0$ (1) holds by (6). Assume (1) holds for l. We have

$$\begin{aligned} z_i^{(l+1)} &= D_i(\boldsymbol{y}^{(l+1)}, \boldsymbol{\phi}^m) \\ &= D_i(\boldsymbol{h}^m, \boldsymbol{\phi}^m) + D_i(\boldsymbol{F}(\boldsymbol{y}^{(l)}), \boldsymbol{\phi}^m)\frac{\tau_m}{2} \\ &= r_i^m + D_i(\boldsymbol{\varepsilon}^m, \boldsymbol{\phi}^m)\frac{\sum_{j=1}^N \varepsilon_j^m \chi_j^m l_\sigma(\nu_j^m)}{\sum_{j=1}^N \varepsilon_j^m z_j^{(l)}}\frac{\tau_m}{2} \\ &\quad - D_i(\boldsymbol{\mu}^{(l)}, \boldsymbol{\phi}^m)\frac{\tau_m}{2}, \end{aligned} \tag{8}$$

where

$$\boldsymbol{\mu}^{(l)} = (\mu_1^{(l)}, \mu_2^{(l)}, \cdots, \mu_N^{(l)}), \quad \mu_i^{(l)} = \frac{\varepsilon_i^m \chi_i^m l_\sigma(\nu_i^m)}{z_i^{(l)}}$$

for $i = 1, 2, \cdots, N$.

By the assumption of induction (1) for l, we have the following estimates for $i = 1, 2, \cdots, N$:

$$\begin{aligned} |D_i(\boldsymbol{\varepsilon}^m, \boldsymbol{\phi}^m)| &\le 2\varepsilon_{\max}^m \frac{1 + |\cos\phi^m|_{\max}}{|\sin\phi^m|_{\min}} \\ &\le \frac{4\varepsilon_{\max}^m}{a_\sigma} = \frac{c_\sigma^m}{b_\sigma}, \\ \left|\sum_{j=1}^N \varepsilon_j^m \chi_j^m l_\sigma(\nu_j^m)\right| &\le \sum_{j=1}^N \varepsilon_j^m l_\sigma(\nu_j^m) \\ &\le (l_\sigma(\nu^m))_{\max} S_\varepsilon^m = b_\sigma S_\varepsilon^m, \\ \left|\sum_{j=1}^N \varepsilon_j^m z_j^{(l)}\right| &\ge z_{\min}^{(l)} S_\varepsilon^m \ge (1-c) r_{\min}^m S_\varepsilon^m, \\ \left|D_i(\boldsymbol{\mu}^{(l)}, \boldsymbol{\phi}^m)\right| &\le \frac{4\mu_{\max}^{(l)}}{a_\sigma} \le \frac{4\varepsilon_{\max}^m (l_\sigma(\nu^m))_{\max}}{a_\sigma z_{\min}^{(l)}} \\ &= \frac{c_\sigma^m}{z_{\min}^{(l)}} \le \frac{c_\sigma^m}{(1-c) r_{\min}^m}. \end{aligned}$$

Here and hereafter we denote $|\mathsf{F}|_{\min} = \min_{1\le i\le N} |\mathsf{F}_i|$ and $|\mathsf{F}|_{\max} = \max_{1\le i\le N} |\mathsf{F}_i|$. Note that from the admissibility and $\psi_i \in (0, \pi)$ for $i = 1, 2, \cdots, N_\sigma$,

$$|\sin\phi^m|_{\min} = a_\sigma \quad \text{and} \quad (l_\sigma(\nu^m))_{\max} = b_\sigma$$

hold for $m = 0, 1, 2, \cdots$.

Therefore $z_i^{(l+1)}$ can be estimated from above and below as follows.

$$\begin{aligned} z_i^{(l+1)} &\le r_{\max}^m + \frac{c_\sigma^m}{b_\sigma}\frac{b_\sigma S_\varepsilon^m}{(1-c) r_{\min}^m S_\varepsilon^m}\frac{\tau_m}{2} + \frac{c_\sigma^m}{(1-c) r_{\min}^m}\frac{\tau_m}{2} \\ &= r_{\max}^m + \frac{c_\sigma^m}{(1-c) r_{\min}^m}\tau_m \\ &\le r_{\max}^m + c r_{\min}^m \le (1+c) r_{\max}^m \end{aligned}$$

and $z_i^{(l+1)} \ge r_{\min}^m - c r_{\min}^m = (1-c) r_{\min}^m$ for $i = 1, 2, \cdots, N$.

(2) By using the estimate (1), we have

$$\begin{aligned} z_i^{(l+1)} - z_i^{(l)} &= D_i(\boldsymbol{\varepsilon}^m, \boldsymbol{\phi}^m) \sum_{j=1}^N \varepsilon_j^m \chi_j^m l_\sigma(\nu_j^m) \\ &\quad \left(\frac{1}{\sum_{j=1}^N \varepsilon_j^m z_j^{(l)}} - \frac{1}{\sum_{j=1}^N \varepsilon_j^m z_j^{(l-1)}}\right)\frac{\tau_m}{2} \\ &\quad - D_i(\boldsymbol{\mu}^{(l)} - \boldsymbol{\mu}^{(l-1)}, \boldsymbol{\phi}^m)\frac{\tau_m}{2}, \\ &\left|\frac{1}{\sum_{j=1}^N \varepsilon_j^m z_j^{(l)}} - \frac{1}{\sum_{j=1}^N \varepsilon_j^m z_j^{(l-1)}}\right| \\ &\le \frac{S_\varepsilon^m ||\boldsymbol{z}^{(l)} - \boldsymbol{z}^{(l-1)}||}{z_{\min}^{(l)} z_{\min}^{(l-1)} (S_\varepsilon^m)^2} \le \frac{||\boldsymbol{z}^{(l)} - \boldsymbol{z}^{(l-1)}||}{((1-c) r_{\min}^m)^2 S_\varepsilon^m}, \\ ||\boldsymbol{\mu}^{(l)} - \boldsymbol{\mu}^{(l-1)}|| &\le \frac{b_\sigma \varepsilon_{\max}^m ||\boldsymbol{z}^{(l)} - \boldsymbol{z}^{(l-1)}||}{z_{\min}^{(l)} z_{\min}^{(l-1)}} \\ &\le \frac{b_\sigma \varepsilon_{\max}^m ||\boldsymbol{z}^{(l)} - \boldsymbol{z}^{(l-1)}||}{((1-c) r_{\min}^m)^2}, \\ \left|D_i(\boldsymbol{\mu}^{(l)} - \boldsymbol{\mu}^{(l-1)}, \boldsymbol{\phi}^m)\right| &\le \frac{4||\boldsymbol{\mu}^{(l)} - \boldsymbol{\mu}^{(l-1)}||}{a_\sigma} \\ &\le \frac{c_\sigma^m ||\boldsymbol{z}^{(l)} - \boldsymbol{z}^{(l-1)}||}{((1-c) r_{\min}^m)^2} \end{aligned}$$

for $i = 1, 2, \cdots, N$.

Hence it holds that

$$\begin{aligned} |z_i^{(l+1)} - z_i^{(l)}| &\le \frac{c_\sigma^m}{b_\sigma} b_\sigma S_\varepsilon^m \frac{||\boldsymbol{z}^{(l)} - \boldsymbol{z}^{(l-1)}||}{((1-c) r_{\min}^m)^2 S_\varepsilon^m}\frac{\tau_m}{2} \\ &+ \frac{c_\sigma^m ||\boldsymbol{z}^{(l)} - \boldsymbol{z}^{(l-1)}||}{((1-c) r_{\min}^m)^2}\frac{\tau_m}{2} = \frac{c_\sigma^m ||\boldsymbol{z}^{(l)} - \boldsymbol{z}^{(l-1)}||}{((1-c) r_{\min}^m)^2}\tau_m \\ &\le c||\boldsymbol{z}^{(l)} - \boldsymbol{z}^{(l-1)}|| \end{aligned}$$

for $i = 1, 2, \cdots, N$.

(3) Since

$$\begin{aligned} y_i^{(l+1)} - y_i^{(l)} &= \left(F_i(\boldsymbol{y}_i^{(l)}) - F_i(\boldsymbol{y}_i^{(l-1)})\right)\frac{\tau_m}{2} \\ &= \varepsilon_i^m \sum_{j=1}^N \varepsilon_j^m \chi_j^m l_\sigma(\nu_j^m)\left(\frac{1}{\sum_{j=1}^N \varepsilon_j^m z_j^{(l)}} - \right. \\ &\quad \left. - \frac{1}{\sum_{j=1}^N \varepsilon_j^m z_j^{(l-1)}}\right)\frac{\tau_m}{2} - \\ &\quad - \varepsilon_i^m \chi_i^m l_\sigma(\nu_i^m)\left(\frac{1}{z_i^{(l)}} - \frac{1}{z_i^{(l-1)}}\right)\frac{\tau_m}{2}, \end{aligned}$$

and

$$\left|z_i^{(l)} - z_i^{(l-1)}\right| = \left|D_i(\boldsymbol{y}^{(l)}, \boldsymbol{\phi}^m) - D_i(\boldsymbol{y}^{(l-1)}, \boldsymbol{\phi}^m)\right|$$
$$\leq \left|\frac{y_{i+1}^{(l)} - y_{i+1}^{(l-1)} - (y_i^{(l)} - y_i^{(l-1)})\cos\phi_i^m}{\sin\phi_i^m}\right|$$
$$+ \left|\frac{y_{i-1}^{(l)} - y_{i-1}^{(l-1)} - (y_i^{(l)} - y_i^{(l-1)})\cos\phi_{i-1}^m}{\sin\phi_{i-1}^m}\right|$$
$$\leq \frac{4}{a_\sigma}||\boldsymbol{y}^{(l)} - \boldsymbol{y}^{(l-1)}||$$

hold for $i = 1, 2, \cdots, N$, we have

$$\left|y_i^{(l+1)} - y_i^{(l)}\right| \leq b_\sigma \varepsilon_{\max}^m S_\varepsilon^m \frac{||\boldsymbol{z}^{(l)} - \boldsymbol{z}^{(l-1)}||}{((1-c)r_{\min}^m)^2 S_\varepsilon^m}\frac{\tau_m}{2} +$$
$$+ b_\sigma \varepsilon_{\max}^m \frac{||\boldsymbol{z}^{(l)} - \boldsymbol{z}^{(l-1)}||}{((1-c)r_{\min}^m)^2}\frac{\tau_m}{2}$$
$$= \frac{2b_\sigma \varepsilon_{\max}^m}{((1-c)r_{\min}^m)^2}||\boldsymbol{z}^{(l)} - \boldsymbol{z}^{(l-1)}||\frac{\tau_m}{2}$$
$$= \frac{a_\sigma c_\sigma^m}{4((1-c)r_{\min}^m)^2}||\boldsymbol{z}^{(l)} - \boldsymbol{z}^{(l-1)}||\tau_m$$
$$\leq c\frac{a_\sigma}{4}||\boldsymbol{z}^{(l)} - \boldsymbol{z}^{(l-1)}||$$

for $i = 1, 2, \cdots, N$, and then

$$||\boldsymbol{y}^{(l+1)} - \boldsymbol{y}^{(l)}|| \leq c\frac{a_\sigma}{4}||\boldsymbol{z}^{(l)} - \boldsymbol{z}^{(l-1)}||$$
$$\leq c||\boldsymbol{y}^{(l)} - \boldsymbol{y}^{(l-1)}|| \leq c^{l-1}||\boldsymbol{y}^{(2)} - \boldsymbol{y}^{(1)}||$$
$$\leq c^l\frac{a_\sigma}{4}||\boldsymbol{z}^{(1)} - \boldsymbol{z}^{(0)}|| \leq c^l\frac{a_\sigma}{4}(||\boldsymbol{z}^{(1)}|| + ||\boldsymbol{z}^{(0)}||)$$
$$\leq c^l\frac{a_\sigma}{4}(2+c)r_{\max}^m \leq c^l r_{\max}^m$$

for $l = 1, 2, \cdots$.

Hence there exist the limits (3).

Remark. $||\boldsymbol{y}^{(l+1)} - \boldsymbol{y}^{(l)}||/r_{\max}^m \leq \delta_{\text{tol}}$ holds if $l \geq \log_c \delta_{\text{tol}}$.

Area-preserving and energy-decreasing properties. From $r_i^m = D_i(\boldsymbol{h}^m, \boldsymbol{\phi}^m)$ and $\boldsymbol{\phi}^{m+1} = \boldsymbol{\phi}^m$, we have

$$\sum_{i=1}^N h_i^m r_i^{m+1} = \sum_{i=1}^N h_i^m D_i(\boldsymbol{h}^{m+1}, \boldsymbol{\phi}^{m+1})$$
$$= \sum_{i=1}^N h_i^m D_i(\boldsymbol{h}^{m+1}, \boldsymbol{\phi}^m)$$
$$= \sum_{i=1}^N h_i^{m+1} D_i(\boldsymbol{h}^m, \boldsymbol{\phi}^m) = \sum_{i=1}^N h_i^{m+1} r_i^m.$$

Let $L_\sigma^m = \sum_{i=1}^N \sigma(\nu_i^m) r_i^m$ be the total interfacial energy on Γ^m. Then, from the above relation, discrete version of $\dot{A} = 0$ and $\dot{L}_\sigma \leq 0$ hold.

Proposition 2.2 *$A^{m+1} = A^m$ and $L_\sigma^{m+1} \leq L_\sigma^m$ hold for $m = 0, 1, 2, \cdots$.*

Proof. From the evolution equation (5), we obtain

$$\frac{A^{m+1} - A^m}{\tau_m} = \frac{1}{2\tau_m}\sum_{i=1}^N \left(h_i^{m+1} r_i^{m+1} - h_i^m r_i^m\right)$$
$$= \frac{1}{2\tau_m}\sum_{i=1}^N \Big(\left(h_i^{m+1} - h_i^m\right) r_i^{m+1} +$$
$$+ h_i^m \left(r_i^{m+1} - r_i^m\right) \Big) =$$
$$= \frac{1}{2\tau_m}\sum_{i=1}^N \left(\left(h_i^{m+1} - h_i^m\right)\left(r_i^{m+1} + r_i^m\right)\right)$$
$$= \sum_{i=1}^N \left(\frac{h_i^{m+1} - h_i^m}{\tau_m} r_i^{m+1/2}\right)$$
$$= 0$$

and

$$\frac{L_\sigma^{m+1} - L_\sigma^m}{\tau_m} = \frac{1}{\tau_m}\sum_{i=1}^N \left(\sigma(\nu_i^{m+1}) r_i^{m+1} - \sigma(\nu_i^m) r_i^m\right)$$
$$= \frac{1}{\tau_m}\sum_{i=1}^N \sigma(\nu_i^m)(r_i^{m+1} - r_i^m)$$
$$= \frac{1}{\tau_m}\sum_{i=1}^N \sigma(\nu_i^m)(D_i(\boldsymbol{h}^{m+1}, \boldsymbol{\phi}^m) -$$
$$- D_i(\boldsymbol{h}^m, \boldsymbol{\phi}^m)) =$$
$$= \sum_{i=1}^N \frac{h_i^{m+1} - h_i^m}{\tau_m} D_i(\boldsymbol{\sigma}(\nu^m), \boldsymbol{\phi}^m)$$
$$= \sum_{i=1}^N \frac{h_i^{m+1} - h_i^m}{\tau_m} k_{\sigma i}^{m+1/2} r_i^{m+1/2}$$
$$\leq 0$$

by using the CBS inequality. The equality holds if and only if $k_{\sigma i}^{m+1/2} = const.$ holds for all i, in other words, $\Gamma^{m+1/2}$ is homothetically the same as the boundary of the Wulff shape W_σ, by the same reason as the continuous case.

How to determine the rescaling sequence $\{R^{(l)}\}_{l=0}^\infty$. Let the l-th length of edge vector in the iteration (5) be $\widetilde{\boldsymbol{z}}^{(l)}$, which is determined from $\widetilde{\boldsymbol{y}}^{(l)} = 2\boldsymbol{y}^{(l)} - \boldsymbol{h}^m$ such as

$$\widetilde{\boldsymbol{z}}^{(l)} = (\widetilde{z}_1^{(l)}, \widetilde{z}_2^{(l)}, \cdots, \widetilde{z}_N^{(l)}),$$
$$\widetilde{z}_i^{(l)} = D_i(\widetilde{\boldsymbol{y}}^{(l)}, \boldsymbol{\phi}^m) = 2D_i(\boldsymbol{y}^{(l)}, \boldsymbol{\phi}^m) -$$
$$- D_i(\boldsymbol{h}^m, \boldsymbol{\phi}^m) = 2z_i^{(l)} - r_i^m$$
$$(i = 1, 2, \cdots, N).$$

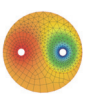

We denote $\widetilde{A}^{(l)}$ by the formal area in the l-th iteration step, which is constructed from $\widetilde{\boldsymbol{y}}^{(l)}$ and $\widetilde{\boldsymbol{z}}^{(l)}$ such as

$$\widetilde{A}^{(l)} = \frac{1}{2}\sum_{i=1}^{N} \widetilde{y}_i^{(l)} \widetilde{z}_i^{(l)}.$$

The following lower estimates hold.

Proposition 2.3 *For $m = 0, 1, 2, \cdots$ and $c \in (0, 1)$ we have the followings.*

$$\begin{aligned}
&(1)\ \widetilde{z}_i^{(l)} \geq (1-c) r_{\min}^m \quad (i = 1, 2, \cdots, N;\\
&\quad l = 0, 1, 2, \cdots).\\
&(2)\ \widetilde{A}^{(l)} \geq (1-c) A^m \quad (l = 0, 1, 2, \cdots).
\end{aligned}$$

Proof. In this proof, we use the definition of λ_m in (7).

(1) Since $z_i^{(0)} = r_i^m$, $\widetilde{z}_i^{(0)} = 2z_i^{(0)} - r_i^m = r_i^m \geq (1-c) r_{\min}^m$ holds for $i = 1, 2, \cdots, N$ and $c \in (0, 1)$. We have the following lower estimate for $\widetilde{z}_i^{(l+1)}$ $(l = 0, 1, 2, \cdots)$ by using (8) and $\lambda \leq 1/2$ in the time increment (7):

$$\begin{aligned}
\widetilde{z}_i^{(l+1)} &= 2z_i^{(l+1)} - r_i^m\\
&= r_i^m + \left(D_i(\boldsymbol{\varepsilon}^m, \boldsymbol{\phi}^m) \frac{\sum_{j=1}^N \varepsilon_j^m \chi_j^m l_\sigma(\nu_j^m)}{\sum_{j=1}^N \varepsilon_j^m z_j^{(l)}} - \right.\\
&\left. - D_i(\boldsymbol{\mu}^{(l)}, \boldsymbol{\phi}^m) \right) \tau_m\\
&\geq r_i^m - \left(\frac{c_\sigma^m}{b_\sigma} \frac{b_\sigma S_\varepsilon^m}{(1-c) r_{\min}^m S_\varepsilon^m} + \right.\\
&\left. + \frac{c_\sigma^m}{(1-c) r_{\min}^m} \right) \tau_m\\
&\geq r_{\min}^m - 2\lambda_m c (1-c) r_{\min}^m\\
&\geq (1-c) r_{\min}^m.
\end{aligned}$$

(2) Since $y_i^{(0)} = h_i^m$ and $z_i^{(0)} = r_i^m$ for $i = 1, 2, \cdots, N$, $\widetilde{A}^{(0)} = \sum_{i=1}^N y_i^{(0)} z_i^{(0)}/2 = \sum_{i=1}^N h_i^m r_i^m/2 = A^m \geq (1-c) A^m$ holds for $c \in (0, 1)$. For $l = 0, 1, 2, \cdots$ we prove $A^m - \widetilde{A}^{(l+1)} \leq cA^m$ as follows.

$$\begin{aligned}
A^m - \widetilde{A}^{(l+1)} &= \frac{1}{2}\sum_{i=1}^N \left(h_i^m r_i^m - \widetilde{y}_i^{(l+1)} \widetilde{z}_i^{(l+1)} \right)\\
&= \frac{1}{2}\sum_{i=1}^N \left((h_i^m - \widetilde{y}_i^{(l+1)}) \widetilde{z}_i^{(l+1)} + \right.\\
&\left. + h_i^m r_i^m - -h_i^m \widetilde{z}_i^{(l+1)}) \right) =\\
&= \frac{1}{2}\sum_{i=1}^N \left((h_i^m - \widetilde{y}_i^{(l+1)}) (\widetilde{z}_i^{(l+1)} + r_i^m) \right)\\
&= \frac{1}{2}\sum_{i=1}^N \left(2(h_i^m - y_i^{(l+1)}) \cdot 2 z_i^{(l+1)} \right)\\
&= -\sum_{i=1}^N F_i(\boldsymbol{y}^{(l)}) z_i^{(l+1)} \tau_m\\
&\leq \left| \sum_{i=1}^N F_i(\boldsymbol{y}^{(l)}) z_i^{(l+1)} \right| \tau_m. \qquad (9)
\end{aligned}$$

Here we have used

$$\begin{aligned}
&\sum_{i=1}^N h_i^m \widetilde{z}_i^{(l+1)}\\
&= \sum_{i=1}^N h_i^m D_i(\widetilde{\boldsymbol{y}}^{(l+1)}, \boldsymbol{\phi}^m)\\
&= \sum_{i=1}^N \widetilde{y}_i^{(l+1)} D_i(\boldsymbol{h}^m, \boldsymbol{\phi}^m) = \sum_{i=1}^N \widetilde{y}_i^{(l+1)} r_i^m.
\end{aligned}$$

The last equation (9) can be estimated as

$$\begin{aligned}
&\left| \sum_{i=1}^N F_i(\boldsymbol{y}^{(l)}) z_i^{(l+1)} \right| \tau_m\\
&= \left| \sum_{i=1}^N \varepsilon_i^m \left(\frac{\sum_{j=1}^N \varepsilon_j^m \chi_j^m l_\sigma(\nu_j^m)}{\sum_{j=1}^N \varepsilon_j^m z_j^{(l)}} \right. \right.\\
&\left. \left. - \frac{\chi_i^m l_\sigma(\nu_i^m)}{z_i^{(l)}} \right) z_i^{(l+1)} \right| \tau_m\\
&\leq \left(\frac{\sum_{i=1}^N \varepsilon_i^m z_i^{(l+1)}}{\sum_{j=1}^N \varepsilon_j^m z_j^{(l)}} \sum_{j=1}^N \varepsilon_j^m b_\sigma + \sum_{i=1}^N \frac{\varepsilon_i^m b_\sigma z_i^{(l+1)}}{z_i^{(l)}} \right) \tau_m\\
&\leq \left(\frac{S_\varepsilon^m (1+c) r_{\max}^m}{S_\varepsilon^m (1-c) r_{\min}^m} S_\varepsilon^m b_\sigma + \frac{S_\varepsilon^m b_\sigma (1+c) r_{\max}^m}{(1-c) r_{\min}^m} \right) \times \tau_m\\
&\leq \frac{2 b_\sigma S_\varepsilon^m (1+c) r_{\max}^m}{(1-c) r_{\min}^m} \times \lambda_m \frac{c(1-c)^2 (r_{\min}^m)^2}{c_\sigma^m}\\
&\leq cA^m
\end{aligned}$$

by using $c_\sigma^m = 4 b_\sigma \varepsilon_{\max}^m / a_\sigma$ and

$$\lambda_m \leq \frac{2\varepsilon_{\max}^m A^m}{a_\sigma (1-c^2) r_{\min}^m r_{\max}^m S_\varepsilon^m}$$

in the time increment (7). Hence we have $A^m - \widetilde{A}^{(l+1)} \le cA^m$.

From Proposition 2.3 (2), we can define

$$R^{(l)} = \sqrt{\frac{A^0}{\widetilde{A}^{(l)}}} \quad (l = 0, 1, 2, \cdots). \tag{10}$$

Therefore, if we put

$$h_i^{(l)} = R^{(l)}\widetilde{y}_i^{(l)}, \quad r_i^{(l)} = R^{(l)}\widetilde{z}_i^{(l)},$$

in the iteration step (5), then the area at the l-th step satisfies

$$A^{(l)} = \frac{1}{2}\sum_{i=1}^{N} h_i^{(l)} r_i^{(l)} = \frac{1}{2}\frac{A^0}{\widetilde{A}^{(l)}}\sum_{i=1}^{N} \widetilde{y}_i^{(l)}\widetilde{z}_i^{(l)} = A^0.$$

Since $h_i^{m+1/2} = (h_i^{m+1} + h_i^m)/2$ and $r_i^{m+1/2} = (r_i^{m+1} + r_i^m)/2$, by the iteration step (5), Proposition 2.1 (3) and Proposition 2.2, we have the following limits as $l \to \infty$:

$$\widetilde{y}_i^{(l)} \to h_i^{m+1}, \quad \widetilde{z}_i^{(l)} \to r_i^{m+1},$$
$$\widetilde{A}^{(l)} \to A^{m+1} = A^m = A^0.$$

The following proposition is specific property of the iteration.

Proposition 2.4 *For $m = 0, 1, 2, \cdots$ we have the following limits*

$$\lim_{l\to\infty} h_i^{(l)} = h_i^{m+1} \quad \textit{and} \quad \lim_{l\to\infty} r_i^{(l)} = r_i^{m+1} \quad (i = 1, 2, \cdots, N),$$

while $A^{(l)} = A^0$ holds in the limit process $l = 0, 1, 2, \cdots$.

How to handle edge-disappearing phenomena. Suppose (A0), (A1), (A2) and $\Gamma^0 = \Gamma_0$, then according to Theorem A, there exists at least one edge Γ_i^m satisfying $\chi_i^m = 0$ and $\liminf_{m\to\infty} r_i^m = 0$ in the case $\varepsilon(\boldsymbol{x}) \equiv 1$. Similarly in the general case $\varepsilon(\boldsymbol{x}) \not\equiv 1$, the edge-disappearing phenomena can be expected, since the function $\varepsilon(\boldsymbol{x})$ just controls how slow-down the normal velocity for each edge. Numerically, we use the following criterion and renumbering steps.

1. Γ^m: given;
2. If there is the minimum number i_0 satisfying $\chi_{i_0}^m = 0$ and $r_{i_0}^m / r_{\max}^m \le \delta_{\text{edge}}$, i.e.,

$$J_N = \left\{ 1 \le i \le N;\ \chi_i^m = 0 \right.$$
$$\left. \text{and } r_i^m / r_{\max}^m \le \delta_{\text{edge}} \right\},$$
$$i_0 = \min\left\{ i \in J_N;\ r_i^m \le r_j^m\ (\forall j \in J_N) \right\},$$

   then GOTO (4);
3. Create Γ^{m+1} according to the scheme, put $m := m + 1$ and GOTO (1);
4. Eliminate the i_0-th edge and shift the number to the j-th edge ($j = 1$) such as

$$\widetilde{N} = N - 2,$$
$$\widetilde{h}_j^{(\mu)} = \begin{cases} (1-\mu)h_{i_0-1}^m + \mu h_{i_0+1}^m & (j = 1) \\ h_{l_j}^m & (2 \le j \le \widetilde{N}) \end{cases},$$
$$\widetilde{\boldsymbol{t}}_j = \boldsymbol{t}_{l_j}^m \quad (1 \le j \le \widetilde{N})$$

   with the periodic boundary conditions $\mathsf{F}_0 = \mathsf{F}_{\widetilde{N}}, \mathsf{F}_{\widetilde{N}+1} = \mathsf{F}_1$, where $l_j = i_0 + j \pmod N$ and μ controls the weighted average of $h_{i_0-1}^m$ and $h_{i_0+1}^m$ defined by (5);

   Compute $\widetilde{\nu}_i$ from $\{\widetilde{\boldsymbol{t}}_j\}_{j=1}^{\widetilde{N}}$ by Construction 1, and compute $\widetilde{r}_i^{(\mu)}$ from $\{\widetilde{h}_j^{(\mu)}\}_{j=1}^{\widetilde{N}}$ and $\{\widetilde{\nu}_j\}_{j=1}^{\widetilde{N}}$ by Construction 2 ($i = 1, 2, \cdots, \widetilde{N}$);
5. Define the intermediate area such as $\widetilde{A}_\mu = \frac{1}{2}\sum_{j=1}^{\widetilde{N}} \widetilde{h}_j^{(\mu)}\widetilde{r}_j^{(\mu)}$ and find μ_* satisfying $\widetilde{A}_{\mu_*} = A^m (= A^0)$ by the bisection method. Since $A^m (= A^0)$ is the value between $\widetilde{A}_0$ and $\widetilde{A}_1$, the bisection method converges as the iteration goes to infinity. Practically, stopping condition of the bisection method is $|\widetilde{A}_\mu - A^m| \le \delta_{\text{area}}$ for $\delta_{\text{area}} > 0$;
6. Put $N := \widetilde{N}$;

   Do renumbering: $h_i^m = \widetilde{h}_i^{(\mu_*)}$, $\nu_i^m = \widetilde{\nu}_i$ ($1 \le i \le N$);
   Compute $\boldsymbol{x}_i^m, \boldsymbol{t}_i^m, \boldsymbol{n}_i^m, r_i^m$ and create Γ^m from $\{h_j^m\}_{j=1}^N$ and $\{\nu_j^m\}_{j=1}^N$ by Construction 2 ($i = 1, 2, \cdots, N$);

   GOTO (1).

Here $\delta_{\text{edge}} > 0$ is a given tolerance for edge-disappearing, and $\delta_{\text{area}} > 0$ is a given tolerance for the bisection method in (5).

3. NUMERICAL COMPUTATION

In this section, we compute (5) for the numerical test of Theorem A, computation starting from the initial setting which is out of the assumption in Theorem A, and for the numerical test of mathematical justification of Nakaya's observation (Ishiwata & Yazaki, 2007, 2008, 2017; Nakaya, 1956). For this purpose we assume the Wulff shape is a regular hexagon, i.e., we assume

$$\sigma \equiv \frac{\sqrt{3}}{2}, \tag{11}$$

and hence we have $l_\sigma \equiv 1$, $\psi_i \equiv \dfrac{\pi}{3}$, $|\phi_i| \equiv \dfrac{\pi}{3}$, and

$$k_{\sigma i} = \frac{\chi_i}{r_i},$$
$$D_i(\mathbf{1}, \boldsymbol{\phi}) = \tan\frac{\phi_i}{2} + \tan\frac{\phi_{i-1}}{2} = \frac{2}{\sqrt{3}}\chi_i \tag{12}$$
$$(i = 1, 2, \cdots, N).$$

Throughout this section, we use the following parameters and the initial area:

$$c = 1/3, \quad \delta_{\mathrm{tol}} = 10^{-13}, \quad \delta_{\mathrm{edge}} = 10^{-3},$$
$$\delta_{\mathrm{area}} = 10^{-13}, \quad A^0 = \bar{\pi}.$$

Here $\bar{\pi}$ is π in the double precision sense. For every numerical computation we have the following precision:

$$|A^m - \bar{\pi}| \leq 10^{-13}.$$

In the following each figure, the far left figure is the initial polygon, and the time evolves from left to right.

3.1. Example of Theorem A

For the numerical test of Theorem A, we put $\varepsilon \equiv 1$.

Figure 1 (upper, far left) is the initial curve. It seems a circle, but it is an almost convex admissible polygon starting with $k_{\sigma i} \geq 0$ for all $i = 1, 2, \cdots, N = 222$. Figure 1 (lower) indicates low number of vertices compared with upper figure. In both figures, all edges which have zero-transition number disappeared step-by-step, and converges to the Wulff hexagon W_σ with $\sigma = \sqrt{3}/2$. These phenomena agree with Theorem A.

The initial polygon of figure 2 (upper, far left) seems rotated figure of the Wulff hexagon, but it is an almost convex admissible polygon starting with $k_{\sigma i} \geq 0$ for all $i = 1, 2, \cdots, N = 594$. The initial figure in figure 2 (lower, far left) is an admissible hexagon with $N = 54$. In both upper and lower figures, numerical evolutions agree with Theorem A.

The final two examples in figure 3 (upper) and (lower) indicate the similar situation above. The initial "triangle" in figure 3 (upper, far left) is not the triangle, but is an admissible almost convex polygonal curve associated with the Wulff hexagon W_σ.

3.2. Example of general setting (4)

For the numerical test of Nakaya's experiments and observation, we use the following function of ε:

$$\varepsilon(\boldsymbol{x}) = \frac{1}{2}\left(1 + \tanh\frac{\boldsymbol{x}\cdot\boldsymbol{e} - c_0}{\delta_{\mathrm{grad}}}\right), \tag{13}$$

where $\delta_{\mathrm{grad}} > 0$ and $c_0 \in \mathbb{R}$ are given parameters, and $\boldsymbol{e}$ is a given unit vector. We have $\varepsilon(\boldsymbol{x}) \to 1$ $(\boldsymbol{x}\cdot\boldsymbol{e} \to \infty)$ and $\varepsilon(\boldsymbol{x}) \to 0$ $(\boldsymbol{x}\cdot\boldsymbol{e} \to -\infty)$. Note that ε approaches Heaviside step function formally when $\delta_{\mathrm{grad}} \to +0$, and c_0 and $\boldsymbol{e}$ control the center and the direction of hyperbolic tangent function. The function ε is a simple role of heat gradient in the ice block. We have used the following parameters:

$$\boldsymbol{e} = (1, 0)^{\mathrm{T}}, \quad c_0 = 0.3, \quad \delta_{\mathrm{grad}} = 0.1.$$

The initial polygons in figure 4 (upper, far left) and (lower, far left) are the same as in figure 1 (upper, far left) and (lower, far left), respectively. Because of the function of ε, the normal velocities of the left side in each figure are almost zero, and the normal velocities of the right side in each figure are almost the same as in velocities in figure 4 (upper) and (lower), respectively. Therefore, almost all edges in the left side do not move, and almost all edges in the right side move and formate toward the Wulff hexagon.

Figure 5 indicates combination of the initial "rotated hexagon" as in figure 2 (Upper, far left) and nontrivial function ε of (13). Left side figure remains as "rotated hexagon" and right side figure converges to the right side of the Wulff hexagon.

3.3. Example of out of Theorem A

The last numerical examples are computation starting from the initial nonconvex polygon as in figure 6 (upper, far left). Theorem A does not cover this example, i.e., we have no theoretical results of asymptotic behavior for nonconvex initial polygon at this stage. From this numerical examples, we can expect convexified phenomena such as the non area-preserving case (Ishiwata, 2008) if we allow the self-intersection.

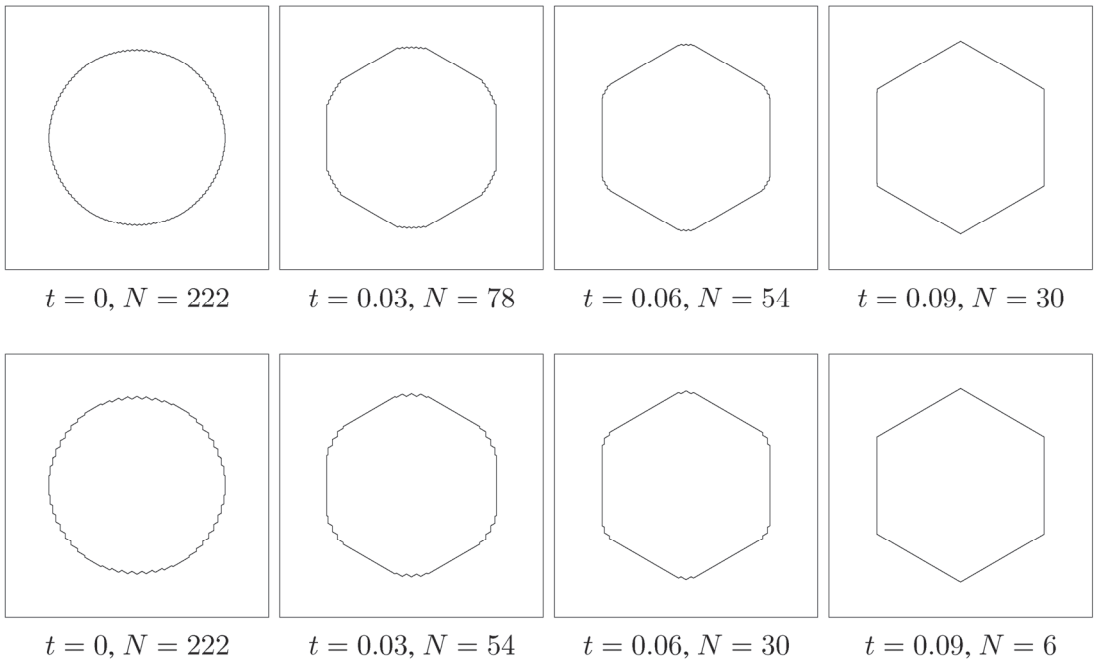

Fig. 1. (Upper) "Circle" to W_σ, starting from $N = 222$, $\varepsilon \equiv 1$. Snapshots are taken at $t = 0, 0.03, 0.06, 0.09$ from left to right. (Lower) Step structured circle to W_σ, starting from $N = 102$, $\varepsilon \equiv 1$. Snapshots are taken at $t = 0, 0.03, 0.06, 0.09$ from left to right.

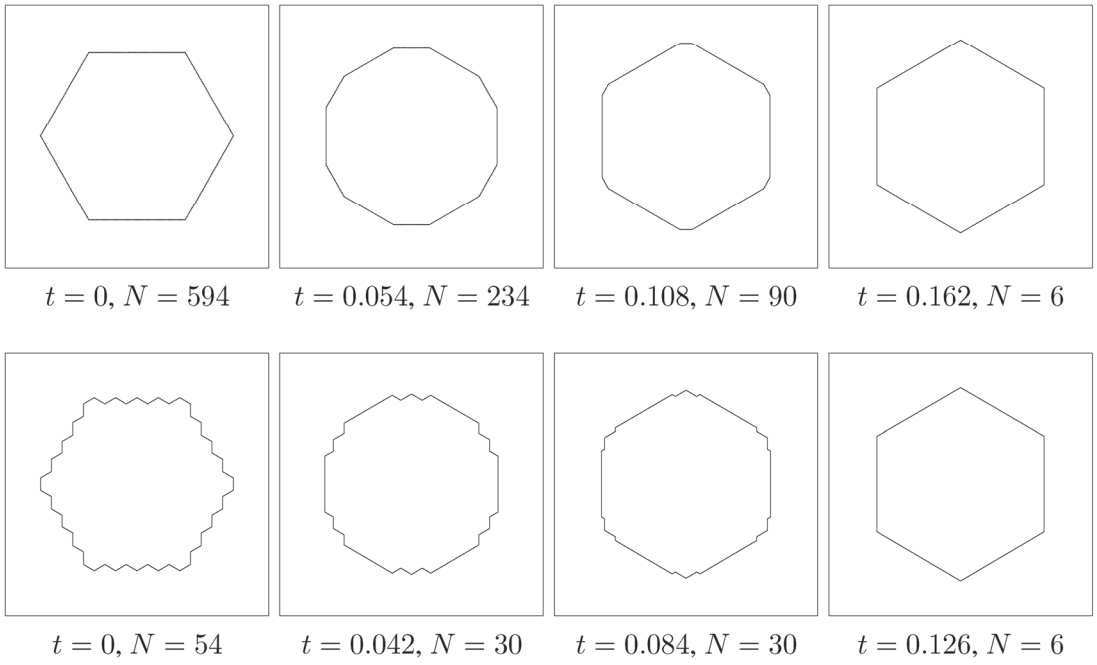

Fig. 2. (Upper) "Rotated W_σ" to W_σ, starting from $N = 594$, $\varepsilon \equiv 1$. Snapshots are taken at $t = 0, 0.054, 0.108, 0.162$ from left to right. (Lower) Admissible hexagon to W_σ, starting from $N = 54$, $\varepsilon \equiv 1$. Snapshots are taken at $t = 0, 0.042, 0.084, 0.126$ from left to right.

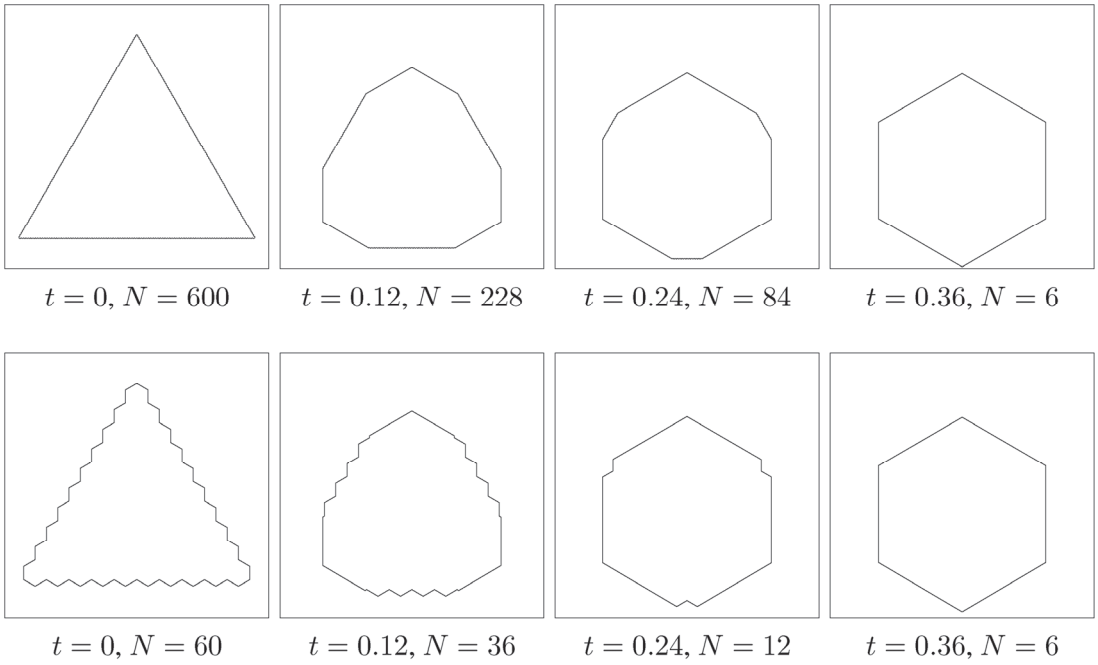

Fig. 3. (Upper) "Triangle" to W_σ, starting from $N = 600$, $\varepsilon \equiv 1$. Snapshots are taken at $t = 0, 0.12, 0.24, 0.36$ from left to right. (Lower) Admissible triangle to W_σ, starting from $N = 60$, $\varepsilon \equiv 1$. Snapshots are taken at $t = 0, 0.12, 0.24, 0.36$ from left to right.

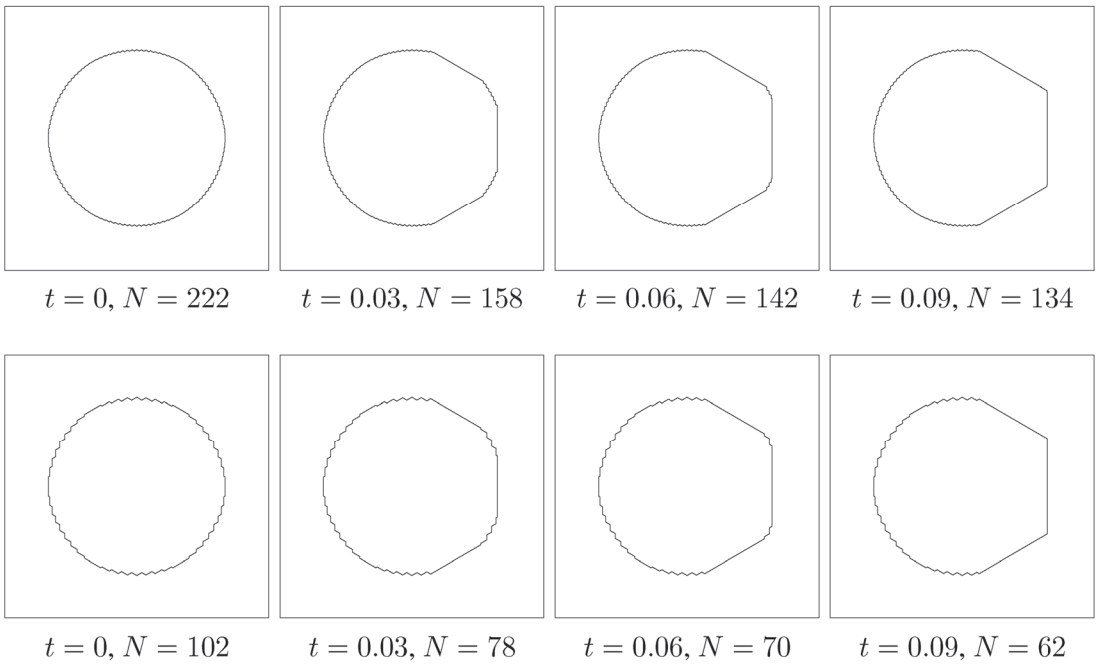

Fig. 4. (Upper) "Circle" to the right half of W_σ, starting from $N = 222$ with ε of (13). Snapshots are taken at $t = 0, 0.03, 0.06, 0.09$ from left to right. (Lower) Step structured circle to the right half of W_σ, starting from $N = 102$ with ε of (13). Snapshots are taken at $t = 0, 0.03, 0.06, 0.09$ from left to right.

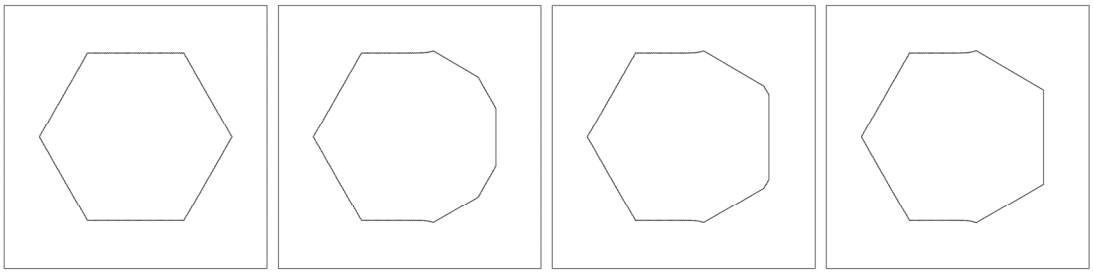

Fig. 5. "Rotated W_σ" to W_σ, starting from $N = 594$ with ε of (13). Snapshots are taken at $t = 0, 0.054, 0.108, 0.162$ from left to right.

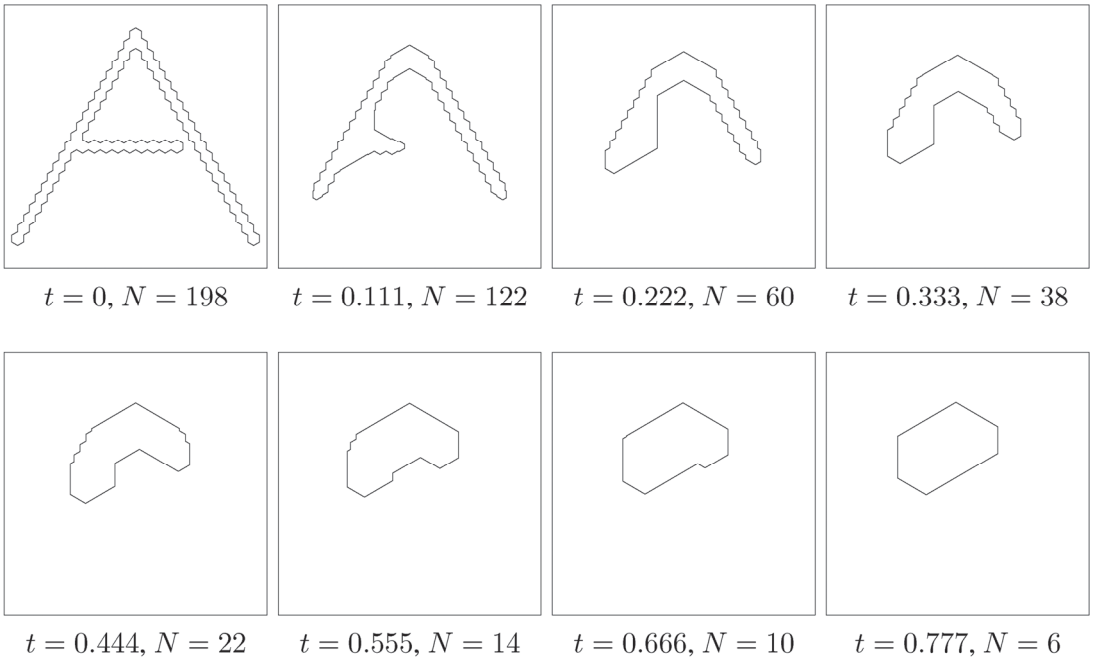

Fig. 6. Capital "A" to hexagon, starting from $N = 198$ with $\varepsilon \equiv 1$. Snapshots are taken at $t = 0, 0.111, 0.222, \cdots, 0.777$ from left to right, from upper to lower.

4. CONCLUSIONS

Accurate numerical scheme for the area preserving crystalline curvature flow was constructed. We verified that the area was preserved in computation within a given accuracy in double precision sense through several numerical examples. Numerical computation were extended from theoretical convexification results starting from almost convex polygon. In particular, Nakaya's experimental observation (Ishiwata & Yazaki, 2007, 2008, 2017; Nakaya, 1956) was justified from numerical point of view.

ACKNOWLEDGEMENTS

The authors are partially supported by KAKENHI (No.15H03632 (TI), No.16H03953 (SY)).

REFERENCES

Angenent, S., Gurtin, M. E., 1989, Multiphase thermo- mechanics with interfacial structure, 2. Evolution of an isothermal interface, *Arch. Rational Mech. Anal.*, 108, 323-391.

Beneš, M., Kimura, M., Yazaki, S., 2009, Second order numerical scheme for motion of polygonal curves with constant area speed, *Interfaces and Free Boundaries*, 11, 515-536.

Ishiwata, T., 2008, Motion of non-convex polygons by crystalline curvature and almost convexity phenom- ena, *Japan J. Indust. Appl. Math.*, 25, 233-253.

Ishiwata, T., Yazaki, S., 2007, Towards modelling the formation of negative ice crystals or vapor figures, *RIMS Kôkyûroku*, 1542, 1-11.

Ishiwata, T., Yazaki, S., 2008, Interface motion of a negative crystal and its analysis, *RIMS Kôkyûroku*,
1588, 23-29.

Ishiwata, T., Yazaki, S., 2017 Convexity phenomena arising in an area-preserving crystalline curvature flow — Nakaya's observation and its mathematical justification, Submitted.

Nayaka, U., 1956, Properties of single crystals of ice, revealed by internal melting, *SIPRE (Snow, Ice and Permafrost Reseach Establishment) Research Pa- per*, 13.

Taylor, J. E., 1991, Constructions and conjectures in crystalline nondifferential geometry, Proceedings of the Conference on Differential Geometry, Rio de Janeiro, *Pitman Monographs Surveys Pure Appl. Math.*, 52, 321-336.

Ushijima, T. K., Yazaki, S., 2004, Convergence of a crystalline approximation for an area-preserving motion, *Journal of Computational and Applied Mathematics*, 166, 427-452.

Yazaki, S., 2002, On an area-preserving crystalline motion, *Calc. Var.*, 14, 85-105.

Yazaki, S., 2007, Asymptotic behavior of solutions to an area-preserving motion by crystalline curvature, *Kybernetika*, 43, 903-912.

Yazaki, S., 2008, An area-preserving crystalline cur- vature flow equation, *Topics in mathematical mod- elling*, Part 4, Jindrich Nec˘as center for mathemat- ical modeling lecture notes eds M. Beneš and E. Feireisl, 4, matfyzpress, 169-215.

ZACHOWUJĄCY STRUKTURĘ SCHEMAT NUMERYCZNY DLA UOGÓLNIONEGO ZACHOWUJĄCEGO POWIERZCHNIĘ KRYSTALICZNEGO RUCHU KRZYWIZNY

Streszczenie

Przedstawiony schemat numeryczny zachowuje zmienną strukturę uogólnionego krystalicznego ruchu krzywizny zachowującego stałą powierzchnię ograniczoną tą krzywizną. Schemat wykorzystuje metody iteracyjną i rzutowania. Szereg numerycznych przykładów potwierdza, że w czasie obliczeń numerycznych niezmienność otoczonej powierzchni jest zachowana z dokładnością podwójnej precyzji. Numeryczne obliczenia potwierdzają teoretyczne wyniki uwypuklenia zaczynając od prawie wypukłego wielokąta i są rozszerzone dla ogólnego układu zaczynając od wklęsłego wielokąta.

Received: June 6, 2017
Received in a revised form: July 31, 2017
Accepted: Sepetember 1,2017